

Optical Studies in ZnS:Ce Nanocrystallite

GEORGE VARUGHESE^{1*} and K. T. USHA²

¹Department of Physics, Catholicate College, Pathanamthitta, Kerala-689645, India

²Department of Chemistry, St. Cyrils College, Adoor, Kerala
gvushakoppara@yahoo.co.in

Received 2 August 2014 / Accepted 5 September 2014

Abstract: Cerium doped ZnS nanoparticles were prepared by chemical route. The particle size was determined from the X-ray line broadening. Samples were characterized by XRD, FTIR and UV and SEM. The composition was verified by EDAX spectrum. The size of the particles increased as the annealing temperature was increased. The crystallite size varied from 21.7 nm to 25 nm as the calcination temperature increased. Band gap values Ce³⁺ doped ZnS were determined to 3.86 eV from the optical transmission studies of the as-prepared samples and exhibited a redshift towards 320 nm in comparison with undoped ZnS nanoparticles. The redshift of the absorption edge to the longer wavelength side has been attributed to the strong exchange interaction between the d electron of Ce and s and p electron of the ZnS host band.

Keywords: Semiconductor, Nanomaterial, Doping, Ultrasonic velocity

Introduction

It is well-known that the optical and electronic properties change dramatically due to quantum confinement of the charge carriers within the particle. ZnS, which is an important wide band gap semiconductor, has potential applications in electronics and optoelectronics including light emitting diodes, efficient phosphors in flat-panel displays and photo voltaic devices because of its wide direct band gap 3.77eV^{1,2}. One Dimensional ZnS nano particle have been attracting growing attention because they possess unique properties compared to bulk crystal due to quantum confinement and surface effect³. Doped semiconductor nanoparticle ZnS:Ce is used as phosphors and also in thin film electroluminescent devices⁴. Recently ZnS nanostructures have shown, a great promise and functional structure nanobuilding blocks in nanoelectronics, nano-optoelectronics and nanolaser^{5,6}. ZnS has been used in many military applications requiring mechanical resistance to hostile environment, missile domes and external windows of military aircraft. Since the mechanical properties are crucial for designing such devices there is an increasing interest in the elasticity of nanostructures. Band gap energy decreases on doping with Ce. The cerium ion doping will change carrier concentration in the ZnS nano particles^{7,8}. The dopant sites, defects induced by doping have strong impact on the Structural, Mechanical and Optical properties of ZnS⁹. Since CeO₂ has a band gap of ~3eV and the fascinating properties that are similar to shows that

of ZnS, the mixed of both materials have been investigated for the probing of highly efficient Photo catalysis¹⁰. The dopant sites defects induced by the doping have strong impact on the structural and optical properties of Ce doped ZnS¹¹. In this paper we report the study on the effect of Ce ion as a dopant in ZnS nanoparticle. The effect of Ce doping on the optical properties was evaluated.

Experimental

Nanoparticles of Ce doped ZnS were prepared by chemical coprecipitation method¹². All the chemicals were of AR grade and were used without further purification. For the synthesis of Ce³⁺ doped ZnS, 3 g (0.35 M) of zinc acetate in 40 mL of deionized water-ethanol matrix (equal volumes) and 1.5 g (0.39 M) of Ce(II) chloride hepta hydrate in 10 mL of water were mixed drop by drop. The entire mixture was stirred magnetically at 80 °C until a homogeneous solution was stirred. The 3 g (1 M) of thiourea in 40 mL of deionized water ethanol matrix was added to the above mixture. The entire solution was stirred magnetically until a white precipitate was formed. The obtained dispersion was purified by dialysis against deionized water and acetone several times to remove impurities. Few drops of Tri Ethyle Amine (TEA) was added to the solution to reduce the agglomeration of particles to remove the impurities, including traces of TEA and the original reactants, if any. The wet precipitate was dried in the controlled temperature furnace at 120 °C for 2 h and thoroughly pulverized.

X-ray diffraction (XRD) and Fourier Transform Infrared (FTIR) analyses of these samples were done for their characterization. XRD patterns were recorded on a RigaKuC/max-2500 diffractometer using graphite filtered CuK α radiation ($\lambda = 1.54056 \text{ \AA}$) at 40 kV and 100 mA with a scanning rate of 8° per min from $2\theta = 5^\circ$ to 80°. The FTIR spectra were recorded in an FTIR spectrometer (Nicolet Magna-750) in the range of 500 cm⁻¹ to 4000 cm⁻¹. The percentage of doped impurity is measured from EDAX spectrum. The Energy Dispersive Analysis of X-rays (EDAX) was done on the sample to ascertain the composition. Scanning Electron Microscopy (SEM) uses electrons to form an image. It is used to show sub-surface defects. In the present study, the UV measurements were done with UV spectrometer JASCO V-550 in the wavelength range of 200 nm to 850 nm. The UV absorption peak of the prepared nanocrystal was measured and computed the optical band with energy.

Results and Discussions

XRD analysis

XRD patterns, of the samples at two different temperatures were carried out. As prepared sample was calcined at 150 and 180 °C for 5 h in air atmosphere to ascertain the formation of different nanocrystalline phases. The patterns are compared with Joint Committee for Powder Diffraction Scan (JCPDS) File No. 01-089-7385. Particle Size, are evaluated and tabulated in Table 1, by the formula^{13,14}, Debye- Scherrer's formula

$$L = K \lambda / \beta \cos \theta \quad (1)$$

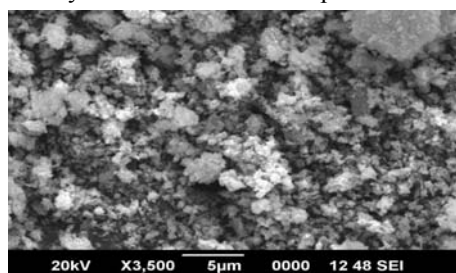
K=0.89, λ the X-ray wavelength = 0.154095 Nm, β the full wavelength at half maximum and θ the half diffraction angle. Particles annealed at temperatures 150 °C and 180 °C have grain sizes 21.7 nm and 25 nm. A continuous increase in the particle size with temperature was observed. According to Ostwald ripening¹⁴ the increase in the particle size is due to the merging of the smaller particles into larger and is a result of potential energy difference between small and large particles and can occur through solid state diffusion. From the X- ray diffraction analysis the crystallite size of Ce³⁺ doped ZnS and undoped ZnS were estimated around 22.7 nm and 5.3 nm respectively. Such an increase in particle size is owing to the broadening of diffraction peaks decreased on cerium doping.

Table 1. Variation of grain size of ZnS:Ce with temperature

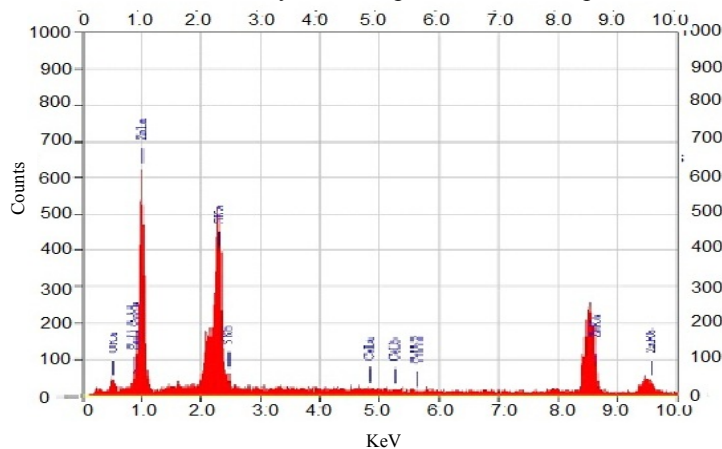
Temperature °C	FWHM	$\beta \times 10^3$	2 θ	θ	Particle size(L) nm
150	0.364	6.34	12.875	6.4375	21.7
180	0.312	5.44	13.352	6.676	25

SEM Image of ZnS:Ce

The morphology, analysis of die/package cracks and fracture surfaces, bond failures, physical defects on the die or package surfaces and dimension of the sample can be studied using SEM. The scanning electron micrographs of ZnS nanomaterials synthesized under aqueous medium. The orientation growth of ZnS crystal in water is higher¹⁵. Spherical shaped morphology is observed in the micrograph of ZnS:Ce (Figure 1). The SEM pictures exhibit spherical morphology with self aligned prismatic nanoparticles. The morphology of ZnS nanopowder as revealed by FESEM showed nanoparticles of size 15-100 Nm.

**Figure 1.** SEM images of the prepared ZnS:Ce nanocrystals*EDAX (EDS) spectrum of ZnS:Ce*

EDS (EDAX) is a technique used for identifying the elemental composition of the specimen. In EDS spectrum, (Figure 2) each of the peaks is unique to an atom, and therefore corresponds to a single element. The higher a peak in a spectrum, the more concentrated the element is in the spectrum. An EDS spectrum plot not only identifies the element corresponding to each of its peaks, but the type of X-ray to which it corresponds as well of our sample. About 97.22% of Zn^{2+} ion and about 2.28% Ce ion by mass are present in the sample.

**Figure 2.** EDAX spectrum of ZnS:Ce nanoparticle

Optical studies

FTIR spectrum of ZnS:Ce

The graph depicted in Figure 3 represents the percentage variation of transmittance with wavenumber (cm^{-1}). For ZnS:Ce annealed at $350\text{ }^{\circ}\text{C}$ the absorption peaks were observed at 3396.15 cm^{-1} , 1625.88 cm^{-1} , 1545.39 cm^{-1} , 1384.10 cm^{-1} , 1019.87 cm^{-1} , 829.06 cm^{-1} , 675.89 cm^{-1} and 608.40 cm^{-1} . The FTIR measurements were undertaken in order to confirm the formation of crystalline ZnS nanoparticle and identify any adsorbed species on to the crystal surface. Bands at 418.56 cm^{-1} is assigned to the stretching vibrations of Zn-S¹⁶. The stretching frequency of bulk ZnS is 483.72 cm^{-1} . Three intense bands are centered at 1384.08 cm^{-1} , 1023.37 cm^{-1} and 1550.06 cm^{-1} and are attributed to the stretching vibrations of C=O, C=C and C-H groups in acetate species, which suggest it presents as adsorbed species in the surface of nanoparticles. The broad absorption peak centered at 3389.47 cm^{-1} and 2922.47 cm^{-1} corresponds to O-H stretching indicating the existence of water in the surface of nanoparticles^{16,17}.

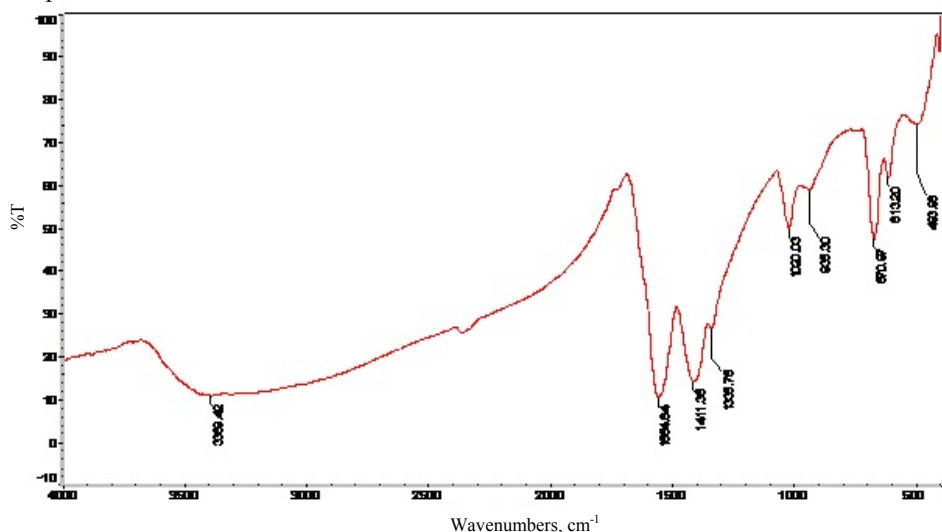


Figure 3. FTIR Spectrum of ZnS:Ce nanoparticle

UV-Vis absorption of ZnS : Ce

From Figure 4, it can be seen that the strongest absorption edge of the prepared sample appears at around 320 nm, which is fairly blue-shifted from the absorption edge of the bulk ZnS (345 nm) and red shifted with respect to undoped ZnS nanoparticle (299 nm). Semiconductor crystallites in the diameter range of a few nanometers show a three dimensional quantum size effect in their electronic structure¹⁸. The relation between absorption coefficient (α) and incident photon energy ($h\nu$) can be written as¹⁹.

$$\alpha = A(h\nu - E_g)^n = h\nu \quad (2)$$

Where A is a constant and E_g is the band gap of the material. Exponent n depends on the type of the transition; n has value $1/2$, as it corresponding to direct transitions. It was noticed that the optical band gap value of undoped ZnS nanoparticle, 4.13 eV, which is higher than the bulk value of ZnS, 3.68 eV¹⁷. From the figure band gap of Ce^{3+} doped ZnS 3.86 eV which can be attributed to the quantum confinement of ZnS nanoparticle.

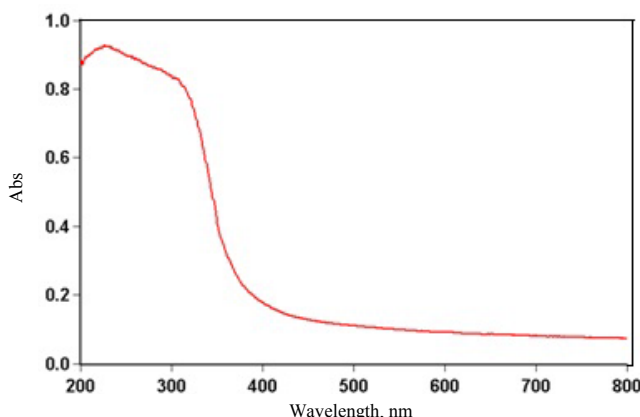


Figure 4. UV- VIS absorption spectrum

The blue shift can be explained on the basis of Burstein-Moss effect. According to which the increase in carrier concentration due to doping of Ce^{3+} results in a shift of the Fermi level and block some of the lowest states, thereby causing widening of the band resulting in the blue shift of the absorption tail. The change in band gap along with exciton features can be used as a measure of particle size and size distribution²⁰. The absorption edge of the Ce^{3+} doped ZnS has been shifted to longer wavelength side, due to the co-valent bonding of Ce with ZnS. As the absorption edge of Ce^{3+} doped ZnS is shifted to longer wavelength, the band gap might be decreased compared to undoped ZnS due to the introduction of new energy in the surface band gap of ZnS nanoparticle¹⁸. The shift of the absorption edge to the longer wavelength side has been attributed to the strong exchange interaction between the *d* electron of Ce and *s* and *p* electron of the ZnS host band²¹. The Ce^{3+} doped ZnS is highly effective and can significantly enhance the photo catalytic degradation¹⁹.

Conclusion

The structure, optical properties, band gap and composition of Ce doped ZnS nanoparticles were determined by XRD, UV-Vis and EDAX spectra analyses. The strongest UV absorption edge appears at around 380 nm, which is fairly blue-shifted from the absorption edge of the bulk (345 nm). The XRD results indicated that the particle size of nano ZnS:Ce is much small as compared to that of pure nano ZnS and increases with the cerium loading. Such an increase in particle size is owing to the broadening of diffraction peaks decreased on cerium doping. From the XRD results, it is clear that as temperature increases, particle size also increases. The change in particle size cause large variation in the physical properties since 1 nm size change may introduce a considerable change in the number of surface atoms with lower coordination and broken exchange bonds. Band gap values Ce doped ZnS were determined to 3.86 eV from the optical transmission studies of the as-prepared samples. The redshift of the absorption edge to the longer wavelength side has been attributed to the strong exchange interaction between the *d* electron of Ce and *s* and *p* electron of the ZnS host band. The UV Absorption spectra show a shift towards 320 nm. The Ce doped ZnS is highly effective and can significantly enhance the photo catalytic degradation.

Acknowledgement

We express our sincere gratitude to the SPAP, M.G University, Kottayam, Kerala for technical support.

References

1. Norris D J. and. Bawendi M G, *Phy Rev B*, 1996, **53**, 16338.
2. Ong H C and Chang R P H, *Appl Phys Lett.*, 2001, **79**(22), 3612-3614.
3. Aruldas N, A Zaben, and A Gadanken, *Chem Mater.*, 1999, **11**(3), 806-813; DOI:10.1021/cm980670s
4. Ye Changhui, Fang Xiaosheng, Li Guanghai and Zhang Lide, *Appl Phys Lett.*, 2004, **85**(15), 3035.
5. Ma C, Moore D and Li J, *Adv Mater.*, 2003, **15**(3), 228-231; DOI:10.1002/adma.200390052
6. Li Q. and Wang, C R, *Appl Phys Lett.*, 2003, **83**, 359; DOI:10.1063/1.1591999
7. Mandal T, Meiti P K and Dasgupta C, *Phys Rev B*, 2012, **86**, 024101.
8. Sridevi P, *J Nano Sci Nano Tech.*, 2014, **2**(1), 34-37.
9. Yan H, Gao M, Wang Y X, Lili Y, Yongjun Z, Jihui L, Dandan W, Huilian L and Hougang F, *Appl Surface Sci.*, 2008, **255**(5), 2646-2650; DOI:10.1016/j.apsusc.2008.08.001
10. Gilbert B, Zhang H, Chan B, Kunz M, Huang F and Banfield J F, *Phy Rev B*, 2006, **74**, 115405
11. Chen H X, Shi D N, Qi J S and Baolin W, *Physica E: Low-dimensional Systems Nanostructures*, 2009, **42**(1), 32-37.
12. Cheng B C, Xiao Y H and Wu G S and Zhang L D, *Adv Funct Mater.*, 2014, **14**, 913-919; DOI: 10.1002/adfm.200305097
13. Peng W Q, Cong, G W Qu, S C and Wang Z G, *Nanotechnology*, 2005, **16**, 1469.
14. Nanda K K, Kruis F E and Fissan H, *Phys Rev Lett.*, 2002, **89**, 256103.
15. Abdul Khader M and Binny Thomas, *Nanostructured Materials*, 1998, **10**(4), 593-600; DOI:10.1016/S0965-9773(98)00100-7
16. Nakamota Kazuo V, (Ed.), *Infrared and Raman spectra of Inorganic and Coordination compounds*, 1972.
17. Sibi Kurian, Shajo Sebastian, Jose Mathew and George K C, *Indian J Pure Appl Phys.*, 2004, **42**, 926.
18. Hou T H, Mao J, Zhu X D and Tu M J, *Rare Met.*, 2006, **25**, 331-336.
19. Lappen P E and Lannoo M, *Phys Rev B*, 1989, **39**(15), 10935; DOI:10.1103/PhysRevB.39.10935
20. Tingting Ren, Holly R and Kristin M |P, *Thin Solid Films*, 2007, **515**, 7976-7983.
21. Laura B L and Christoffer O K, *Chem Mater.*, 1997, **9**(6), 1302-1317; DOI:10.1021/cm960441a